Technical Note

Noninvasive Acoustic Cell Trapping in a Microfluidic Perfusion System for Online Bioassays

Mikael Evander, Linda Johansson, Tobias Lilliehorn, Jure Piskur, Magnus Lindvall, Stefan Johansson, Monica Almqvist, Thomas Laurell, and Johan Nilsson

Anal. Chem., **2007**, 79 (7), 2984-2991 • DOI: 10.1021/ac061576v

Anal. Chem. **2007,** *79,* 2984−2991

Noninvasive Acoustic Cell Trapping in a Microfluidic Perfusion System for Online Bioassays

Mikael Evander,*,† Linda Johansson,‡ Tobias Lilliehorn,‡ Jure Piskur,§ Magnus Lindvall,⊥ Stefan Johansson,‡ Monica Almqvist,† Thomas Laurell,† and Johan Nilsson†

Department of Electrical Measurements, Department of Cell and Organism Biology, and Department of Child and Adolescent Psychiatry, Lund University, Lund, Sweden, and Department of Engineering Science, Uppsala University, Uppsala, Sweden

Techniques for manipulating, separating, and trapping particles and cells are highly desired in today's bioanalytical and biomedical field. The microfluidic chip-based acoustic noncontact trapping method earlier developed within the group now provides a flexible platform for performing cell- and particle-based assays in continuous flow microsystems. An acoustic standing wave is generated in etched glass channels (600 × 61 μm^2) by miniature ultrasonic transducers (550 × 550 × 200 μm^3). Particles or cells passing the transducer will be retained and levitated in the center of the channel without any contact with the channel walls. The maximum trapping force was calculated to be 430 ± 135 pN by measuring the drag force exerted on a single particle levitated in the standing wave. The temperature increase in the channel was characterized by fluorescence measurements using rhodamine B, and levels of moderate temperature increase were noted. Neural stem cells were acoustically trapped and shown to be viable after 15 min. Further evidence of the mild cell handling conditions was demonstrated as yeast cells were successfully cultured for 6 h in the acoustic trap while being perfused by the cell medium at a flowrate of 1 μL/min. The acoustic microchip method facilitates trapping of single cells as well as larger cell clusters. The noncontact mode of cell handling is especially important when studies on nonadherent cells are performed, e.g., stem cells, yeast cells, or blood cells, as mechanical stress and surface interaction are minimized. The demonstrated acoustic trapping of cells and particles enables cell- or particle-based bioassays to be performed in a continuous flow format.

The global industrial standard for large-scale cell-based assays utilizes the 96 or 384 microtiter plate format.[1]Transparent microtiter plate well arrays enable high-throughput optical readout. A frequently raised question in regards to well-based cell assays is the relevance of this model system as compared to the corresponding biological in vivo situation. A major concern relates to the metabolic turnover of the well-based system as no continuous exchange of metabolites and nutrients prevail, unlike the in vivo situation. In regards to this, it has been expressed that it is difficult to control the microenvironment within the wells, especially for slowly growing organisms that require long incubation times.[2] Another aspect is the fact that microtiter plates are not ideal when working with nonadherent cells, which are better processed in a wall-less environment.

It has been demonstrated that cell assays are preferably performed using perfusion-based systems, since they ensure a stable microenvironment by providing fresh nutrients and removing metabolites.[3,4] Perfusion systems have now been improved by miniaturization,[5] which has resulted in, for instance, smaller sample volumes, higher sensitivity, faster readouts, and excellent fluid control.[6] By moving cell assays down to the microscale, the laminar flows within the microfluidic channels provide controlled transportation of cells, analytes, and cell medium. Furthermore, the overall cell consumption can be lowered since techniques exist that enable handling of a few or single objects. Finally, microfluidic systems can be automated and are more easily integrated with further analysis steps.[7]

However, to be able to perform assays in a perfusing system a technique for controlled trapping or holding of the cells in a flow is needed, allowing the execution of a given set of chemical and/or microfluidic unit operations. This can be performed by seeding cells on the bottom of microfluidic culture wells or channels[8,9] or by using a contact method, e.g., patch−clamp.[10] Alternatively, noncontact methods for levitating objects within a

* To whom correspondence should be addressed. Phone: +46-46-222 75 27. Fax: +46-46-222 45 27. E-mail: Mikael.evander@elmat.lth.se.

† Department of Electrical Measurements.

‡ Department of Engineering Science.

§ Department of Cell and Organism Biology.

⊥ Department of Child and Adolescent Psychiatry.

(1) Mann, R. Presented at MipTec-ICAR'99, Montreux, 1999.
(2) Kumar, S.; Wittmann, C.; Heinzle, E. *Biotechnol. Lett.* **2004**, *26*, 1−10.
(3) Powers, M. J.; Janigian, D. M.; Wack, K. E.; Baker, C. S.; Stolz, D. B.; Griffith, L. G. *Tissue Eng.* **2002**, *8*, 499−513.
(4) Kim, L. Y.; Lee, H.-Y.; Voldman, J. *Micro Total Analysis Systems*; Transducer Research Foundation: Boston, 2005; pp 530−532.
(5) Hung, P. J.; Lee, P. J.; Sabounchi, P.; Lin, R.; Lee, L. P. *Biotechnol. Bioeng.* **2005**, *89*, 1−8.
(6) Petersen, K. E.; McMillan, W. A.; Kovacs, G. T. A.; Northrup, M. A.; Christel, L. A.; Pourahmadi, F. *Biomed. Microdevices* **1998**, *1*, 71−79.
(7) Andersson, H.; van der Berg, A. In *Lab-on-Chips for Cellomics*; Andersson, H., van der Berg, A., Eds.; Kluwer Academic Publishers: Dordrecht, 2004, pp 1−22.
(8) Yu, H. M.; Meyvantsson, I.; Shkel, I. A.; Beebe, D. J. *Lab Chip* **2005**, *5*, 1089−1095.
(9) Price, A. K.; Fischer, D. J.; Martin, R. S. *Anal. Chem.* **2004**, *76*, 4849−4856.
(10) Olofsson, J.; Pihl, J.; Sinclair, J.; Sahlin, E.; Karlsson, M.; Orwar, O. *Anal. Chem.* **2004**, *76*, 4968−4977.

10.1021/ac061576v CCC: $37.00
Published on Web 02/22/2007

microfluidic environment can be employed, which is especially advantageous for nonadherent cells. For multistep assays, either several trapping sites are required or a fluidic system that not only allows for fast fluid exchange but also for rapid transport of the particles/cells between trapping sites without losses. It is also important to be able to address each trapping site with individual fluids so as to avoid any contamination or carryover from earlier steps.

Presently, several techniques that all rely on different physical phenomena are used to concentrate and trap cells, many of which are well suited for integration in a miniaturized system. These techniques include optical tweezers, dielectrophoretic trapping, and methods based on ultrasonic fields. Optical tweezers were developed by Ashkin[11] in the 1970s and use a focused laser beam to create forces, originating from the photon radiation pressure, sufficiently strong to trap and hold a micrometer-sized particle or cell.[12] By calibrating the system it can be used for quantitative measurements of biological forces on a cellular level. The trapped object can be translated with extremely high precision, and by rapidly scanning the laser beam between different positions, several particles or cells can be held by a single laser beam. Although optical tweezers is a high-precision technique, it can only be used on a limited number of cells, and the position of the cell needs to be known in advance. To trap and hold larger cell clusters would demand a higher number of lasers leading to a very complex system. Care must also be taken to avoid absorption of laser light by trapped cells, since this may result in a dramatic temperature increase and cell damage. The forces acting on the trapped object are in the vicinity of 100 pN depending on the intensity of the laser beam.[12,13]

Dielectrophoretic trapping utilizes a nonuniform electric field that exerts an electrostatic force on polarizable particles or cells.[14,15] The particles can either be moved toward the high-intensity parts of the field, i.e., positive dielectrophoresis, or toward the low, i.e., negative dielectrophoresis. This differential reaction to a field can be used for trapping combined with separation and preconcentration. The effect of the dielectrophoretic forces is decided by the electrode shape and layout, as shown by Duschl et al.[16] This enables a multitude of particle manipulation tasks to be performed on the same chip by defining varying electrode geometries in the channels. Although it is a very versatile technique, it requires polarization of the manipulated object. Moreover, to design the system correctly, the frequency at which the object will experience positive or negative dielectrophoresis must also be known. There is also a risk of cell damage from the stress induced by the electrical field or joule heating if care is not taken when designing the system.[17] The applied forces are typically in the range of a couple of hundred pico-Newtons.[18]

The ultrasonic techniques usually use an ultrasonic standing wave to create a pressure node that will attract particles or cells. As with dielectrophoresis, a cell can experience either an attractive or repellent acoustic force depending on its material parameters.[19] This can be used either to trap objects locally over an ultrasonic transducer,[20] concentrate them within a fluidic channel, or separate different types of objects from each other.[21] Ultrasound has been used for many years in macroscale resonators using rather low frequencies, thus resulting in low trapping forces and without the advantage of the microfluidic networks.[22] The effect of the acoustic pressure on cells in ultrasonic traps at moderate frequencies has also been studied intensively.[23−25]

Integrating an array of miniature ultrasonic transducers in a microfluidic channel, matched for operations in the 10 MHz regime, will give localized trapping with a high trapping force compared to that of the macroscale systems commonly working at lower frequencies. Advanced fluid control by means of integrated microfluidics makes it possible to create a perfusion-based system with individually addressable trapping sites that can handle small populations of cells in a noncontact mode. The basic characteristics of such a system were described by Lilliehorn and co-workers in 2005,[26,27] targeting controlled trapping of microbeads and perfusion-based bioassays.

We now demonstrate that the further developed acoustic trapping platform also is capable of handling live cells. The overall system design is improved by integrating the channel and the reflector into a single glass unit. This results in high geometric precision, which is essential in a resonant system. The trapping force was calculated using a single trapped particle in a fluid flow. Accurate temperature control in the trap was accomplished by characterizing the power dissipation in relation to the transducer driving voltage. The question whether the employed acoustic field is influencing cells negatively was addressed by a viability test of trapped neural stem cells and by culturing yeast cells for 6 h.

MATERIALS AND METHODS

Acoustic Forces. When an object enters an acoustic standing wave a force will act on it, forcing it to either the pressure node or the pressure antinode depending on the material parameters. The primary radiation force (F_{PRF}, see the inset in Figure 1a) acting on a compressible sphere in an acoustic standing wave field

(11) Ashkin, A. *IEEE J. Sel. Top. Quantum Electron.* **2000**, *6*, 841−856.
(12) Molloy, J.; Padgett, M. *Contemp. Phys.* **2002**, *43*, 241−258.
(13) Qian, F.; Ermilov, S.; Murdock, D.; Brownell, W. E.; Anvari, B. *Rev. Sci. Instrum.* **2004**, *75*, 2937−2942.
(14) Gonzalez, C. F.; Remcho, V. T. *J. Chromatogr., A* **2005**, *1079*, 59−68.
(15) Huang, Y.; Ewalt, K. L.; Tirado, M.; Haigis, R.; Forster, A.; Ackley, D.; Heller, M. J.; O Connell, J. P.; Krihak, M. *Anal. Chem.* **2001**, *73*, 1549−1559.
(16) Duschl, C.; Geggier, P.; Jäger, M.; Stelzle, M.; Müller, T.; Schnelle, T.; Fuhr, G. R. In *Lab-on-Chips for Cellomics*; Andersson, H., van der Berg, A., Eds.; Kluwer Academic Publishers: Dordrecht, 2004; pp 83−122.
(17) Menachery, A.; Pethig, R. *IEE Proc: Nanobiotechnol.* **2005**, *152*, 145−149.
(18) Taff, B. M.; Voldman, J. *Anal. Chem.* **2005**, *77*, 7976−7983.
(19) Petersson, F.; Nilsson, A.; Holm, C.; Jonsson, H.; Laurell, T. *Analyst* **2004**, *129*, 938−943.
(20) Wiklund, M.; Toivonen, J.; Tirri, M.; Hanninen, P.; Hertz, H. M. J. *Appl. Phys.* **2004**, *96*, 1242−1248.
(21) Coakley, W. T. *Trends Biotechnol.* **1997**, *15*, 506−511.
(22) Groschl, M. *Acustica* **1998**, *84*, 632−642.
(23) Bazou, D.; Kuznetsova, L. A.; Coakley, W. T. *Ultrasound Med. Biol.* **2005**, *31*, 423−430.
(24) Wang, Z.; Grabenstetter, P.; Feke, D. L.; Belovich, J. M. *Biotechnol. Prog.* **2004**, *20*, 384−387.
(25) Ryll, T.; Dutina, G.; Reyes, A.; Gunson, J.; Krummen, L.; Etcheverry, T. *Biotechnol. Bioeng.* **2000**, *69*, 440−449.
(26) Lilliehorn, T.; Simu, U.; Nilsson, M.; Almqvist, M.; Stepinski, T.; Laurell, T.; Nilsson, J.; Johansson, S. *Ultrasonics* **2005**, *43*, 293−303.
(27) Lilliehorn, T.; Nilsson, M.; Simu, U.; Johansson, S.; Almqvist, M.; Nilsson, J.; Laurell, T. *Sens. Actuators, B* **2005**, *106*, 851−858.

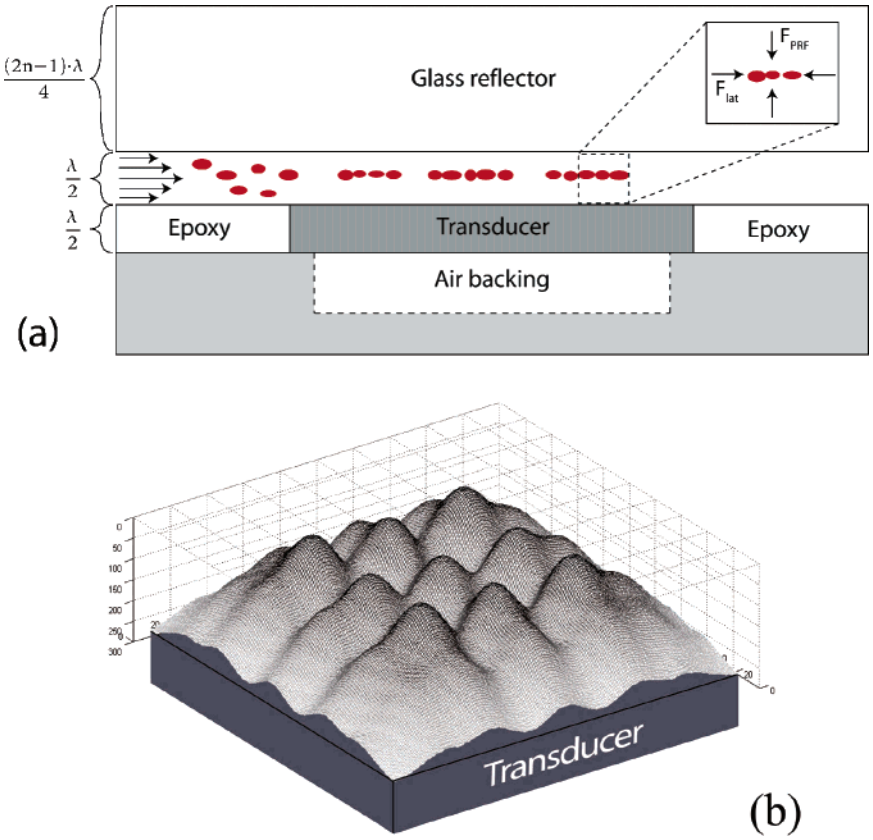

Figure 1. (a) Side-view schematic of the microfluidic device. The glass reflector with etched fluidic channels is clamped to the PCB holding the transducer. Cells infused into the chip are trapped in the ultrasonic standing wave formed in the channel. The acoustic forces focus the cells into clusters in the center of the channel as illustrated in the inset. (b) Since the trapping occurs close to the transducer surface, the actual trapping sites are given by the near-field pressure distribution as shown in the 3D image. Cells will be trapped in clusters around the local pressure minima creating different patterns depending on the amount of cells trapped. The peaks in the graph correspond to the pressure minima.

was described by King[28] and Gorkov[29] and can be seen in eq 1:[30]

$$F_{\mathrm{PRF}} = \frac{-\pi P_0^{\,2} V \beta_0}{2\lambda} \sin\left(\frac{4\pi z}{\lambda}\right)\left(\frac{(5\rho_{\mathrm{p}} - 2\rho_0)}{(2\rho_{\mathrm{p}} + \rho_0)} - \frac{\beta_{\mathrm{p}}}{\beta_0}\right) \qquad (1)$$

The equation is based on a spherical particle with volume V, compressibility β_{p}, and density ρ_{p} suspended in a fluid with compressibility β_0 and density ρ_0. The particle is situated in an acoustic standing wave with wavelength λ and will experience a force that will increase with higher frequency or larger volume. Most microparticles and cell types will be forced to the pressure nodes by the primary radiation force, whereas, for instance, lipid particles will be drawn to the pressure antinodes.[31] The primary radiation force can, depending on the device design, either be used to position objects or to trap them.[32]

Whereas the primary radiation force will move the particles into the pressure node, see the inset in Figure 1, it does not prevent the particles from moving laterally within the nodal plane itself. Lateral forces (F_{LAT}), arising due to spatial variations in the pressure field and acoustic streaming,[33,34] will, however, keep the particles positioned at stable positions within the nodal plane. The actual trapping position are governed by the local pressure distribution over the transducer, as shown by Lilliehorn et al.[26] An inverted 3D image showing the simulated local pressure minima over the transducer, i.e., the trapping positions, is shown in Figure 1b. There are also secondary forces,[35] created by pressure waves being reflected on particles, that drive the particles to form clusters, helping to stabilize the trapped objects. Thus, the trapped particles will form patterns consisting of clusters positioned at or close to the local pressure minima. The lateral distribution of the clusters will change depending on the frequency and amount of particles being trapped.

Acoustic Resonator Design and Fluidic Channel Fabrication. The microfluidic device is composed of a base plate of a printed circuit board, PCB, providing electrical connection to the ultrasonic transducers. An array of three in-house-developed miniature PZT transducers,[36] 550 × 550 × 200 μm^3, is mounted on the PCB and cast in epoxy as illustrated in Figure 1. A glass

(28) King, L. V. *Proc. R. Soc. London* **1934**, *A147*, 212−240.
(29) Gorkov, L. P. *Sov. Phys. Dokl.* **1962**, *6*, 773−775.
(30) Whitworth, G.; Coakley, W. T. *J. Acoust. Soc. Am.* **1992**, *91*, 79−85.
(31) Petersson, F.; Nilsson, A.; Holm, C.; Jönsson, H.; Laurell, T. *Lab Chip* **2005**, *5*, 20−22.
(32) Wiklund, M.; Spegel, P.; Nilsson, S.; Hertz, H. M. *Ultrasonics* **2003**, *41*, 329−333.
(33) Woodside, S. M.; Bowen, B. D.; Piret, J. M. *AIChE J.* **1997**, *43*, 1727−1736.
(34) Spengler, J. F.; Coakley, W. T. *Langmuir* **2003**, *19*, 3635−3642.
(35) Gröschl, M. *Acustica* **1998**, *84*, 432−447.
(36) Lilliehorn, T.; Johansson, S. *J. Micromech. Microeng.* **2004**, *14*, 702−709.

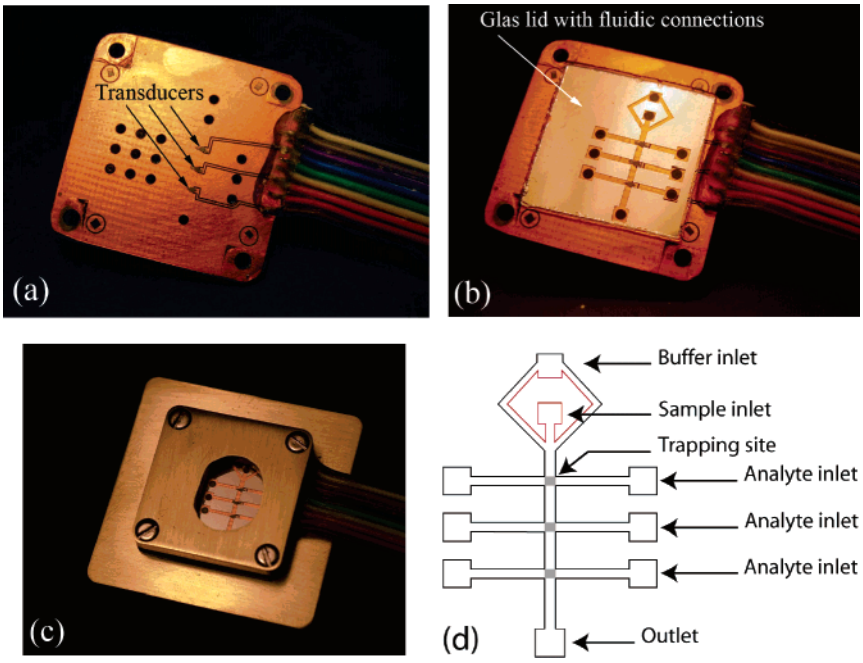

Figure 2. Microfluidic acoustic resonator is based on a PCB with three miniature PZT transducers, 550 × 550 μm^2 (a). The PCB provides fluidic and electric connections to the transducers. A glass lid with microfluidic channels placed over the PCB defines the resonator cavity over each transducer (b), and the entire assembly is fixed by a brass holder (c). A schematic of the channels with the transducers, i.e., trapping sites, marked with gray (d).

lid with etched microchannels, 600 μm wide and 61 μm deep, is placed on the PCB and acts as a matched acoustic reflector and provides optical access to the trapping sites. The complete assembly of the acoustic device is shown in Figure 2. Silicone tubings, 1 mm i.d., provide fluidic connections to standard 1.58 mm o.d. Teflon tubings on the back side of the PCB, allowing for particle or cell injections assisted by a pressure-driven carrier flow. Channels orthogonal to the main channel enable individual perfusion of each trapping site, see Figure 2d.

To form a standing wave with a pressure node in the center of the channel, the depth of the channel is typically designed to be a half-wavelength. The reflector should be an odd multiple of a quarter of a wavelength in order to achieve a completely reflected wave.[37] The device used in viability and trapping experiments was designed to work at the transducer resonance of 12.4 MHz giving the fluidic channels a depth of 61 μm to create a $\lambda/2$ resonator in water and thus creating the trapping zone in the center of the channel. For the device used in the temperature measurements the drive frequency differed slightly,[41]12.2 MHz, due to slight individual variations for transducers and channel structures.

The microfluidic device, earlier described by Lilliehorn et al.,[26] used spin-coated and photolithography-patterned polymeric materials, SU-8 and polyimide, to define the microfluidic channels. These materials showed problems with swelling when subjected to prolonged exposure to ultrasound and water. The swelling changed the channel depth, resulting in a mismatched acoustic resonance system. As a consequence, a loss in trapping efficiency was seen over time. Furthermore, it was difficult to achieve the submicrometer precision needed to be able to match the channel depth to the frequency of the desired ultrasound.

In this paper wet etching of the channels in glass was rather used, which provided the good reproducibility and high level of dimensional control required. Thereby, long-term operation of the microfluidic acoustic trapping system was enabled, which was crucial for the cell culturing experiments performed.

Instrumentation. An Agilent 33120A waveform generator was used to actuate the transducers with a sinusoidal signal at 12.4 MHz and an amplitude of 7 Vpp. All cell pictures were taken with a Hamamatsu ORCA CCD on an Olympus BX51WI fluorescence microscope. The fluid was driven by a SP210IWZ syringe pump (World Precision Instruments, Inc., Sarasota, FL) using Hamilton glass syringes. The fluorescence temperature measurements were performed with an inverted Nikon TE2000 epifluorescence microscope and an SE6 Monochrome CCD camera.

Particle Trapping Efficiency. The trapping performance of the device with respect to particle size and trapping efficiency has been evaluated using polystyrene particles ranging in size from 0.87 to 10 μm in diameter.

High trapping efficiency is important when manipulating cells in samples with low abundance. In acoustic applications the trapping efficiency is essentially given by the percentage of injected cells collected in the acoustic trap. In a design where side channels are used there is always a risk of losing some cells which bypass the trapping area, due to the widening flow profile in the side-channel intersection. Therefore, by hydrodynamically focusing the sample flow at the inlet,[38] the overall trapping efficiency can be improved by directing the cell sample over the center of the transducer.

To determine the effect of hydrodynamic focusing on the trapping efficiency, a particle suspension was infused into the chip with and without hydrodynamic focusing. The number of particles passing the transducer was manually counted while a sample, containing approximately 2000 particles, was infused at two

(37) Hawkes, J. J. *Proc. Forum Acusticum 2002* Sevilla 2002.

(38) Kenis, P. J. A.; Ismagilov, R. F.; Whitesides, G. M. *Science* **1999**, *285*, 83–86.

different flow rates. The hydrodynamically focused injection used two different sample injection flow rates, 1 and 3 μL/min, and a focusing flow of 3 μL/min. The unfocused injection used a sample injection flow of 1 and 3 μL/min and no focusing flow. The particles used were 10 μm polystyrene beads in a suspension of MilliQ water with 20% glycerol added to reduce sedimentation. The particles were injected for 30 s using the lower flow rates and for 20 s using the higher flow rate. For each flow rate the experiment was repeated six times, and the mean and standard deviation were calculated.

Trapping Force. In order to compare the ultrasonic trapping to other trapping techniques the lateral trapping force was measured. The lateral forces acting on the trapped objects will determine the maximum useable fluid velocities.

By relating the drag force exerted from the fluid flow to the retaining ultrasonic force a measure of the lateral trapping force was provided. A similar method was used by Tuziuti et al.[39] showing good agreement with theory.

The drag force acting on a single spherical particle in a laminar flow is described by Stoke's law, eq 2,

$$F = 3\pi\mu D_p v \tag{2}$$

where μ denotes the fluid viscosity, D_p is the particle diameter, and v is the fluid velocity.

The particle Reynolds number was calculated to be around 10^{-8}, which is very well below the limit of 2, making the use of Stoke's law valid.[40]

To relate the trapping force to the drag force a very dilute particle suspension was injected using hydrodynamic focusing. A single 10 μm particle was trapped at an initial flow of 1 μL/min (0.42 mm/s) as specified by a syringe pump. After the particle was trapped the particle injection flow was switched off. The focusing flow was increased in steps of 1 μL/min until the particle was pulled away from the trapping site, i.e., when the fluidic drag force exceeded the lateral trapping force. The maximum linear flow velocity was calculated from the volume flow with the channel cross section and the parabolic flow profile taken into account. The trapping was performed at a frequency of 12.4 MHz and an amplitude of 7 Vpp. The drag force was calculated for the last fluid velocity at which the particle was still trapped and used as a measure of the lateral acoustic force on the particle.

Temperature Measurements. Sudden temperature changes or prolonged exposure to too low or too high temperatures may cause irreversible harm to live cells. During activation of the transducers, the piezoelectric material displays mechanical and dielectric losses which may cause a temperature rise in the fluidic channel through thermal conduction. Absorption of the acoustic energy in the fluid layer will also yield a temperature rise in the channel. The temperature increase in the fluid channel was evaluated as a function of the driving voltage at the transducer resonance frequency.[41]

By using a temperature-dependent fluorescent dye, an accurate temperature sensing can be achieved in microfluidic systems[42] without affecting the ultrasonic field. Rhodamine B was used due to the easy handling and high-temperature sensitivity in the interval of 0−120 °C.[43] A calibration curve was generated by measuring the fluorescent intensity in the channel at a set of temperatures and calculating the median gray-scale intensity in each image. A linear curve fit was made in the region of 0−13 °C temperature increase relative to a reference temperature of 24.8 °C. The measured parameter is the average temperature data in the channel. To be able to account for parameters that may vary over time, such as lamp intensity, the image median were normalized to room-temperature data.

A solution of 0.1 mM rhodamine B was infused at 0.5 μL/min into the system, and the fluorescent readout was monitored during ultrasonic radiation using a fluorescent microscope (Inverted Nikon TE2000 epifluorescence microscope, Hg lamp, SE6 Monochrome CCD camera, Spot Software, 30× objectives, and 8 bit images). During calibration, a Peltier element was used to heat the chip and was mounted on the brass holder in contact with the glass channel. The device was embedded in polymer foam to minimize heat losses. A thermocouple type K (Pentronic G/G-36-K) was mounted with silicone paste (Wacker silicone heat sink paste P12) in contact with the channel for temperature readings on a thermometer display (Line Seiki thermometer TC-1200, with a resolution of 0.1 °C). After activating the transducer, a stable temperature was observed for 2 min before opening the aperture and recording an image. A linear fit[42] was made within the temperature region of 0−11 °C of temperature increase, and the standard deviation within this region was 0.3 °C.

The temperature increase in the channel due to power dissipation from the transducer can, as a first approximation, be described by Fourier's law which assumes a linear relation between heat flow, G [W•s^{-1}•m^{-2}], and a temperature difference, ΔT, over a given distance:

$$G = -k\frac{\Delta T}{\Delta x} \tag{3}$$

where k is the thermal conductivity [J•m^{-1}•s^{-1}•K^{-1}]. If the power dissipation from the transducer will be conductively transported through the fluid and the temperature at the reflector surface is constant, then the relation between the power dissipation and the temperature increase in the channel will be linear.

The temperature response on a voltage change is expected to be quadratic since a quadratic voltage dependence is found for the acoustic power from a transducer[44] as well as for mechanical[45] and dielectric losses[46] under the assumption that nonlinearities in the material are ignored.

(39) Tuziuti, T.; Kozuka, T.; Mitome, H. *Jpn. J. Appl. Phys., Part 1* **1999**, *38*, 3297−3301.

(40) Coulson, J. M.; Richardson, J. F. In *Particle Technology and Separation Processes*, 4th ed.; Pergamon: Oxford, 1991; Vol. 2, p 98.

(41) Johansson, L.; Nilsson, M.; Lilliehorn, T.; Almqvist, M.; Nilsson, J.; Laurell, T.; Johansson, S. *Proc.—IEEE Ultrason. Symp.* **2005**, 1614−1617.

(42) Ross, D.; Gaitan, M.; Locascio, L. E. *Anal. Chem.* **2001**, *73*, 4117−7123.

(43) Lou, J. F.; Finegan, T. M.; Mohsen, P.; Hatton, T. A.; Laibinis, P. E. *Rev. Anal. Chem.* **1999**, *18*, 235−284.

(44) Berlingcourt, D. A.; Kreuger, H. H. A. Behaviour of Piezoelectric Ceramics under Various Environmental and Operation Conditions of Radiating Sonar Transducers. www.morganelectroceramics.com/pdfs/tp228.pdf (accessed March 21, 2006).

(45) Sherrit, S.; Bao, X.; Sigel, D. A.; Gradziel, M. J.; Askins, S. A.; Dolgin, B. P.; Bar-Cohen, Y. *IEEE Ultrason. Symp., Proc.* **2001**, 1097.

(46) Moulson, A. J.; Herbert, J. M. In *Electroceramics: Materials, Properties, Applications*; Chapman & Hall: London, 1990; p 230.

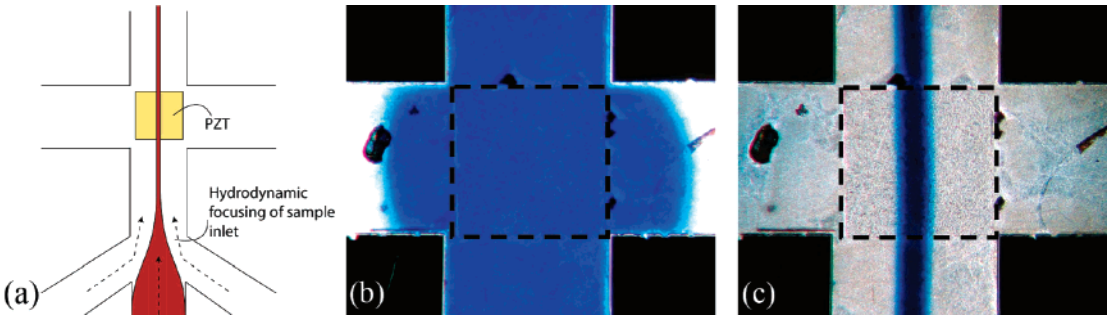

Figure 3. (a) Schematic setup for focusing the particle or cell flow over the transducer center. In (b) the flow profile of an unfocused dye infused over the transducer (outlined) can be seen, and in (c) the dye is hydrodynamically focused and is kept over the transducer center. A focused cell injection prevents loss of cells due to the widened flow profile at the channel cross section.

Table 1. Influence of Hydrodynamic Focusing on the Trapping Efficiency[a]

	no. of particles lost with focusing	no. of particles lost without focusing
low flow	1.33 ± 1.97	26.8 ± 13.3
high flow	0.67 ± 0.82	62.8 ± 13.1

[a] A sample containing approximately 2000 particles was infused into the device. The number of particles passing the transducer was manually counted with and without hydrodynamic focusing. When a focused injection was used, a clear improvement was noted, which was even more pronounced at higher flow rates.

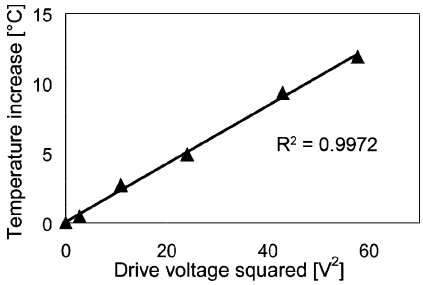

Figure 4. Measured temperature increase relative to room temperature in the fluid volume above the transducer surface as a function of the squared drive. The linear curve fit confirms the expected quadratic behavior of the power loss terms.

Biological Material. To investigate how cells respond to being suspended in the high-frequency ultrasonic standing wave, three cell experiments were performed.

An initial cell-trapping experiment was performed using spleen cells from rats, fluorescently marked using acridine orange.

The yeast strain, *Saccharomyces cerevisiae* UMR 106 (MATα LEU2-VENUS ade2-1 can1-100 his3-11,15 ura3-1 lys2-deletion), from U. Mortensen's collection (Technical University of Denmark, Denmark) was used in the subsequent cell culturing experiment. This yeast strain has an ORF coding for yellow fluorescent protein (YFP) (Venus) attached in frame to the LEU2 gene. To achieve maximal signal strength from the yeast cells, the defined synthetic cell medium without leucin, SC-Leu,[47] was used. The trapped cells were perfused with the cell medium at a rate of 1 μL/min, and images of the cell cluster were taken every hour during 6 h.

The cells used in the viability assay were a rat neural stem cell line from embryonic hippocampus, HiB5-GFP,[48] genetically modified to express green fluorescent protein (GFP). The cell medium used was standard phosphate-buffered saline solution (PBS) with a pH of 7.4. After 15 min of PBS perfusion, a viability marker, acridine orange, was supplied through an orthogonal side channel, testing the cell cluster for viability while still suspended in the acoustic trap. Fluorescent images were taken before and after the perfusion of the viability marker to determine whether or not it had migrated into the cells.

RESULTS AND DISCUSSION

Particle Trapping Efficiency. The trapping was very weak using 0.87 μm particles, whereas 1.8 μm particles and larger were easily trapped. This corresponds well to eq 1, stating that larger particles experience a larger trapping force, making them easier to trap. The largest particle diameter possible to handle in a half-wavelength resonator is practically determined by the geometrical dimensions of the microfluidic channels.

A comparison between a hydrodynamically focused and an unfocused dye injection can be seen in Figure 3. The use of hydrodynamic focusing made it possible to direct the sample inlet over the center of the transducer. This avoids loss of particles that bypass the trapping area due to the widening flow profile in the side-channel intersection. Further, the risk of losing particles has experimentally been seen to be higher when the trapping occurs near the edges of the transducer.

Generally, the trapping efficiency is very high for all cases, see Table 1. However, an increase in the number of lost particles can be seen in the case without focusing, and at higher flow rates the advantage of the focused sample injection is more apparent. The particles not trapped at the higher flow rates passed the transducer at the side channels due to the widened flow profile.

Without the hydrodynamic focusing there is a risk that particles or cells are retained in the side channels, and in a sample with low abundance of cells it is crucial not to lose any biological material. Any cells caught in the side channels may also affect the following steps in an analysis by carryover, making the hydrodynamic focusing an important step.

Trapping Force Estimation Using Single-Particle Trapping. The resulting mean trapping force from 16 consecutive measurements was calculated to be 430 ± 135 pN, which corresponds to a maximum fluid velocity of 4.6 ± 1.4 mm/s. For each measurement a single 10 μm particle was trapped at approximately the same position over the transducer surface and held against an increasing fluid flow until it was displaced from

(47) Piskur, J.; Kielland-Brandt, M. C. *Biotechnol. Appl. Biochem.* **1993**, *18*, 239–257.
(48) Renfranz, P. J.; Cunningham, M. G.; McKay, R. D. G. *Cell* **1991**, *66*, 713–729.

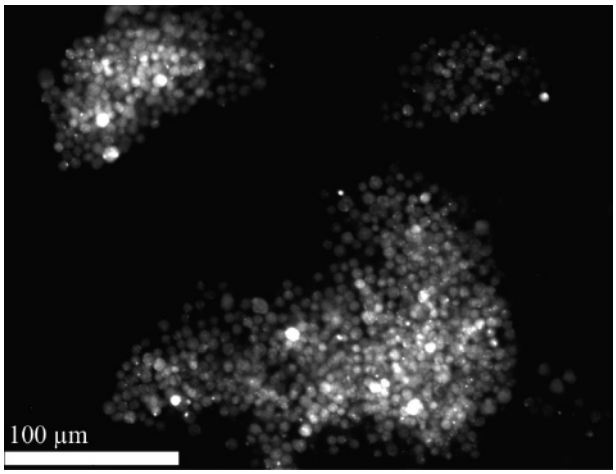

Figure 5. Subsection of the trapping area showing trapped clusters of rat spleen cells that are held against a fluid flow to investigate cell-trapping behavior. The cells were fluorescently marked with acridine orange to improve visibility.

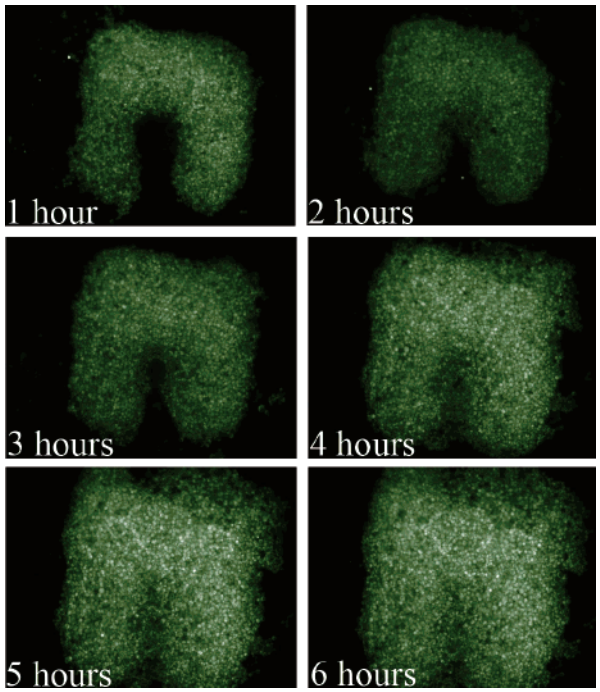

Figure 6. Growth of YFP-expressing yeast cells, UMR106, trapped in the acoustic device while being perfused with cell medium. The images show the increase of the number of cells in the cell cluster after 1−6 h of cultivation. The successful growth indicates that the cell proliferation is not affected by the high-frequency acoustic radiation. The horseshoe-shaped pattern is caused by the cells clustering in the near-field pattern.

the transducer. The depth-wise position of each particle was given by the pressure node in the center of the channel. The lateral position of the studied particles was visually confirmed to be in the same near-field pressure node. The trapping force was calculated using eq 2 with the fluid velocity noted immediately before the bead disappeared from the trap.

The acoustic trapping force can be compared to optical tweezers, which usually works in the 100 pN range,[12,13] and dielectrophoretic devices that work in the ranges of 400−500 pN.[18] Direct comparisons between the different techniques are however

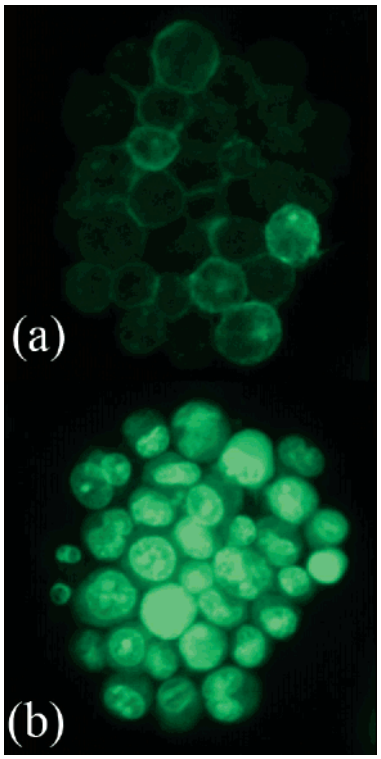

Figure 7. Viability assay on a cluster of acoustically trapped neural stem cells, HiB5-GFP, modified to express green fluorescent protein, GFP. The cells were exposed to 15 min of continuous ultrasonic radiation and were then perfused with acridine orange through the side channels as a test for viability. In (a) the cells are shown shortly after being trapped, and in (b) the cells have been subjected to 15 min of continuous ultrasonic radiation in the trap, after which they were perfused with acridine orange. The acridine orange has migrated into the cells, indicating a viable cell cluster. The exposure time of the camera is approximately 6 times longer in (a), demonstrating the dramatic fluorescence increase of the cells after acridine orange resorption in (b). Only a very small shape and rotational change of the cell cluster can be seen after 15 min of trapping.

not possible since the material parameters and device design strongly affect the forces.

Temperature Measurements. Increasing the driving voltage resulted in an accelerated temperature increase as expected, and the quadratic behavior between temperature increase and voltage corresponded well to theory, see Figure 4. At a drive voltage of 7 Vpp, at which level several transducers showed good trapping with 5 μm polystyrene particles, the temperature increase was 7.2 °C yielding an absolute temperature of 30.0 °C.

Since the temperature increase is dependent on the voltage over the transducer, it is possible to tune the channel temperature to a certain degree by changing the actuation amplitude of the transducer. This can be used to create microenvironments suitable for many cell types using the same device.

Cell Experiments. Three types of live cell experiments were performed to study the possibility of carrying out live cell assays. The first experiment was conducted with spleen cells from rats and was primarily aimed at trapping and holding live cells in the acoustic standing wave. The cells were trapped instantaneously as the ultrasound was activated while perfused by buffer. Part of the trapping area, showing three trapped cell clusters, can be seen in Figure 5. As the ultrasound was deactivated the cells were immediately released and removed from the trapping site by the

buffer flow, showing that the trapping did not occur at the channel walls. Thus, a continuously perfused noncontact cell trapping was accomplished.

In the second experiment, yeast cells expressing yellow fluorescent protein (YFP) under the control of the LEU2 gene promoter were maintained and grown in the acoustic trap for 6 h to ensure that no long-term effects resulted from the acoustic forces on live cells. The cells were continuously perfused with the cell medium to promote growth, and images were taken every hour for 6 h, see Figure 6. The successful cell growth clearly indicates that the acoustic environment does not affect the cell proliferation. Therefore, it can be anticipated that this device can be used to study proliferation of cells as a function of different media. For example, a study of the response time of yeast cells to changes in their microenvironment could be performed.

Finally, a viability test was performed on acoustically levitated neural stem cells, HiB5-GFP, see Figure 7. The cells were trapped and exposed to acoustic forces for 15 min. The viability test was performed while the cells were still suspended in the standing wave by administrating acridine orange through the side channel. The cells showed no perceptible damage from the acoustic radiation and responded well to the viability test, as indicated by the increase in fluorescence caused by the active transport of the acridine orange into the cells.

The cell experiments indicate that the ultrasonic environment within the standing wave does no perceptible harm to live cells. Future work will include longer acoustic exposure combined with the exposure to different media and analysis of the mutability effect.

CONCLUSIONS

Noncontact trapping and retention of cells in microfluidic networks by means of acoustic standing wave forces are demonstrated as a platform for perfusion-based cell handling and assaying. The current improvements of the described acoustic trapping microfluidic platform provide stable resonator dimensions over extended periods of operation. A key feature is the manufacturing of the microfluidic channels directly in the glass reflector layer, thus avoiding the use of photolithography-defined polymer gaskets that may undergo swelling during the experiments. This now enables longer periods of stable operation of the noncontact acoustic particle/cell trapping platform as demonstrated in the cell culturing experiment over 6 h. The temperature measurements indicate that the thermal environment in the acoustic trap is at a level where no negative effects are expected on cell behavior. The viability tests verify that the acoustic intensities used give no indication of being harmful to the cells, but this will have to be confirmed by extended studies, including gene expression profile analysis.

In future work, the possibility of single-cell trapping will enable the study of growth and response of single cells under the influence of various environmental conditions as set by the perfusing fluids. We are currently targeting further studies in noncontact microfluidically controlled cell-based assays. The upscaling to multiple trapping sites in an array format will further provide the ability to either generate statistical data on multiple identical experiments or the possibility to run screening protocols with concentration gradients of a given substance. It will also enable efficient analysis of the cell response to different substances from a library. A further outlook is to link this cell-based trapping and chemostimulation platform to the nanoproteomic chip technologies developed earlier in our group,[49] enabling differential protein expression mapping of small cell populations due to the integrated and confined microfluidic format.

ACKNOWLEDGMENT

This work has been supported by the Swedish Foundation for Strategic Research and the Crafoord Foundation.

SUPPORTING INFORMATION AVAILABLE

A video sequence of trapping of hydrodynamically focused fluorescent microparticles. This material is available free of charge via the Internet at http://pubs.acs.org.

Received for review August 23, 2006. Accepted January 3, 2007.

AC061576V

(49) Ekström, S.; Wallman, L.; Hök, D.; Marko-Varga, G.; Laurell, T. *J. Proteome Res.* **2006**, *5*, 1071−1081.